

Anticancer Properties of Actinomycetes-Derived Secondary Metabolites on the MCF-7 Breast Cancer Cell Line: Cytological and Molecular Investigations

Basma Nasr Hassan^{1*}, Ahmed Said El Azzuni¹, Mohamed Saleh Abdelfattah², Mohamed Sayed Elgabri¹, Asmaa Salah Ahmed¹, Sara Mohamed Abdo²

¹Department of Chemistry, Faculty of Science, Helwan University, Cairo, Egypt.

²Department of Zoology and Entomology, Faculty of Science, Helwan University, Cairo, Egypt.

*E-mail ✉ basmanasr@science.helwan.eg

Received: 10 October 2023; Revised: 14 December 2023; Accepted: 18 December 2023

ABSTRACT

Heliomycin, a compound obtained from the secondary metabolites of actinomycetes bacteria, was tested for its anticancer effects, with tamoxifen serving as the reference drug. Flow cytometry, cell cycle analysis, and apoptosis assays were performed, alongside real-time RT-PCR to evaluate gene expression. The expression of CK-19 was examined by immunocytochemistry, while cytopathological changes were observed using H&E staining and electron microscopy. The results of real-time PCR showed that HER-2 expression was lower in tamoxifen-treated cells compared to those treated with heliomycin. In contrast, the P53 gene showed a significant increase in expression in the heliomycin group, compared to both the tamoxifen-treated and control groups. On the other hand, the genes ER α , TNF α , and TLR-4 showed decreased expression in heliomycin-treated cells. The apoptosis assays showed a significant increase in both early and late apoptotic cell populations in cells treated with either tamoxifen or heliomycin when compared to the control group. Examination by H&E staining and electron microscopy confirmed cell apoptosis, chromatin fragmentation, and shrinkage in the treated groups, whereas such effects were not observed in the control group. Immunohistochemistry of CK-19 showed strong expression in control cells, moderate expression in tamoxifen-treated cells, and mild expression in heliomycin-treated cells. Overall, heliomycin showed promising anticancer effects by inducing apoptosis and upregulating tumor suppressor genes in MCF-7 breast cancer cells.

Keywords: Tumour suppressor gene, Breast cancer, Heliomycin, Cell culture, Chemotherapy

How to Cite This Article: Hassan BN, El Azzuni AS, Abdelfattah MS, Elgabri MS, Ahmed AS, Abdo SM. Anticancer Properties of Actinomycetes-Derived Secondary Metabolites on the MCF-7 Breast Cancer Cell Line: Cytological and Molecular Investigations. Asian J Curr Res Clin Cancer. 2023;3(1):63-76. <https://doi.org/10.51847/oc4COUq6V>

Introduction

Breast cancer is the most commonly diagnosed type of cancer and a leading cause of cancer-related deaths worldwide [1]. In Egypt, breast cancer is the most prevalent malignancy, accounting for 18.9% of all cancer cases [2]. Common symptoms of breast cancer include nipple discharge, redness or changes in the breast's appearance, or alterations in its texture. Early detection through regular breast exams is crucial for preventing the disease from spreading [3].

Chemotherapy and surgery remain the primary treatment methods for breast cancer [4]. However, chemotherapy faces challenges due to the toxicity of the drugs and the development of resistance [5]. Tamoxifen, a well-established anti-estrogen drug, has been in use for over 40 years and remains a cornerstone of breast cancer treatment [6].

A significant proportion of approved drugs are derived from natural sources, with over 60% of them originating from nature [7]. Among these, 50% are natural antibiotics derived from actinomycetes, which are also recognized for their antifungal, antibacterial, and anti-inflammatory properties [8]. Despite this, there is a lack of sufficient

research on the potential anti-cancer properties of metabolites derived from marine actinomycetes-based drugs. Actinomycetes, often found as symbiotic microbes, are commonly associated with marine sponges [9], making them excellent sources for discovering new bioactive compounds [10]. Various natural substances derived from marine sponge-associated actinomycetes have been evaluated for their anticancer properties against different cancer cell lines [11]. One such promising secondary metabolite is heliomycin, produced by marine bacteria [12]. Breast cancer cell lines, particularly MCF7 and MDA-MB-231, are widely used in basic research due to their significant contributions to understanding breast cancer biology [13]. These cell lines are vital for identifying new therapeutic targets and studying the signaling pathways involved in breast cancer development [14]. MCF7 and MDA-MB-231 cells represent invasive ductal breast cancer, but they exhibit distinct phenotypic and genetic differences: MDA-MB-231 is a triple-negative breast cancer cell line, while MCF7 is hormone-dependent (positive for estrogen and progesterone receptors) [15]. The objective of our study was to assess the anticancer potential of heliomycin in breast cancer treatment.

Materials and Methods

Reagents and chemicals

The following chemicals were sourced from Sigma-Aldrich (USA): RPMI-1640 medium, trypsin (0.25%), fetal bovine serum (FBS), penicillin, streptomycin, and ethanol. Tamoxifen, the chemotherapeutic agent, was obtained from AstraZeneca (UK). The secondary metabolite, heliomycin, derived from actinomycetes, was identified at the Marine Natural Products Unit (MNPRU) of Helwan University, as outlined in Abdelfattah *et al.* [10]. MCF-7 cells, a human breast cancer cell line, were acquired from VACSERA Holding Company, Egypt. Cultureware was supplied by TPP, Switzerland.

Cell culture conditions

The MCF-7 cell line was cultured in RPMI-1640 medium enriched with 10% FBS, penicillin (100 U/ml), streptomycin (100 µg/ml), 20 mM HEPES, and 25 mM sodium bicarbonate. The cells were incubated in a humidified incubator at 37 °C as previously described [16].

Heliomycin extraction and isolation

Actinomycetes strains were isolated and identified according to the methods in Abdelfattah *et al.* [17].

Preparation of drug solutions

The heliomycin extract was dissolved in dimethyl sulfoxide (DMSO) to prepare a 10 mg/ml stock solution. Tamoxifen tablets were powdered and dissolved in DMSO to achieve a 10 mg/ml concentration.

Cytotoxicity testing

The cytotoxic effects of heliomycin and tamoxifen on MCF-7 cells were assessed using the MTT assay. Cells were seeded in 96-well plates and cultured for 24 hours. Following incubation, various concentrations of the drugs were applied, and cells were further incubated for 24 hours. The untreated cells served as negative controls. Microscopic examination was performed to detect cell degeneration. The degenerated cells were washed with PBS (ADWIA, Egypt). MTT was then added to the viable cells at 0.5 mg/ml and incubated for 4 hours. The cells were analyzed using a BIOTEK ELx-800 Plate ELISA reader at 570 nm, and the IC₅₀ values were calculated using Master Plex-2010 software.

Assessment of anticancer activity

For the anticancer evaluation, MCF-7 cells were treated with the calculated IC₅₀ concentrations of heliomycin and Tamoxifen, with untreated cells acting as controls. After 24 hours of incubation, cells were examined for morphological changes under a microscope. Detached cells were removed by washing with PBS. The adherent cells were harvested by trypsinization, centrifuged at two thousand rpm for ten minutes, and washed with cold PBS. The resulting cell pellets were resuspended in 100 µl of PBS, labeled, and stored at -70 °C for further analysis.

Real-time PCR procedure

Total RNA was isolated from the cells utilizing the RNeasy Plus Mini Kit (Qiagen, Valencia, CA), following the manufacturer's protocol. The extracted RNA was then used for the synthesis of complementary DNA (cDNA), applying the RevertAid™ H Minus Reverse Transcriptase enzyme (Thermo Fisher Scientific Inc., Fermentas, Canada). For gene expression analysis, the cDNA samples were amplified in triplicate. Quantitative real-time PCR (qRT-PCR) was conducted using Power SYBR® Green Master Mix (Life Technologies, CA) on an Applied Biosystems 7500 Real-Time PCR System, ensuring accurate amplification and detection of target genes. As an internal reference, β -actin was used. The arithmetic formula $2^{-\Delta\Delta CT}$ was used to calculate relative mRNA quantification. Primer sequences for the studied genes are as follows HER2 F:5'-GGT CCT GGA AGC CAC AAG G-3'. R: 5'-GGT TTT CCC ACC ACA TCC TCT-3' p53, F, 5'- CCCCTCCTGGCCCCCTGTCATCTTC-3', R: 5'-GCAGCGCCTCACAACCTCCGTCAT-3' TNF- α F: 5'-CTT CAG GGA TAT GTG ATG GAC TC-3'R: 5'- GGA GAC CTC TGG GGA GAT GT -3' ER- α F, 5'-TCCTGGACAAGATCACAGAC-3' R: 5'-GGT TTT CCC ACC ACA TCC TCT-3', TLR-4 F: 5'-TTGAAGACAAGGCATGGCATGC-3' R: 5'-TCTCCAAGATCAACCGATG-3', β -actin, F; 5'-TGACGGGGTCACCCACACTGTGCCCATCTA-3' R; 5'CTAGAAGCATTGCGGTGGACGATGGAGGG-3'

Flow cytometry and cell cycle analysis

Both adherent and suspended MCF-7 cells were harvested and subjected to two sequential washes with phosphate-buffered saline (PBS) to remove residual media. The evaluation of apoptosis was conducted using the Annexin V-FITC/propidium iodide (PI) apoptosis detection kit (ab139418, BD Biosciences), following the instructions provided by the manufacturer. Cells were initially incubated with Annexin V conjugated to fluorescein isothiocyanate (FITC) for 5 minutes. Following this step, PI staining was performed by incubating the cells in darkness for an additional 10 minutes. Flow cytometric analysis was then carried out using a fluorescence-activated cell sorter (FAC), and the collected data were processed using Cell Quest software (Becton–Dickinson, USA) to determine the apoptotic cell population and analyze the cell cycle distribution [18].

Cytopathological analysis

To prepare samples for cytological examination, 50 μ l of cells treated with heliomycin or tamoxifen were carefully applied onto clean glass slides, with three replicates allocated for each experimental group. The slides underwent a dehydration process through graded ethanol solutions (100%, 90%, 75%, and 50%), air-dried thoroughly, and then fixed with methanol. Slides were subsequently rinsed with distilled water for 5 minutes. Hematoxylin staining was performed for 3 minutes, followed by two washes with distilled water. Thereafter, slides were briefly (5 seconds) immersed in eosin stain and washed again. After complete drying, the slides were cleared using xylene, mounted with Canada balsam, and covered with coverslips. Microscopic examination was conducted using a light microscope connected to a digital camera (Canon, Japan), and images were captured at 400x magnification from ten selected fields per slide. The chosen fields were determined based on the density of apoptotic cells. Photomicrographs were qualitatively analyzed for the presence of morphological characteristics typical of apoptosis.

Immunocytochemistry

For immunocytochemical detection, MCF-7 cell monolayers grown on glass slides were initially stabilized using 10% neutral buffered formalin. Following fixation, the cells were exposed to the primary antibody anti-CK19 (Labvision, Neomarkers, USA) for 90 minutes to target cytokeratin 19 expression. This was succeeded by the application of a secondary antibody using the Vectastain ABC kit (Vector Laboratories, Burlingame, CA), with detection performed via the immunoperoxidase staining protocol.

Transmission electron microscopy (TEM)

To prepare MCF-7 cells for ultrastructural analysis, cells were harvested by centrifugation at 2000 rpm for 10 minutes. The resulting cell pellets were immersed in 3% glutaraldehyde prepared in 0.1M sodium cacodylate buffer (pH 7.0) for two hours at ambient temperature. Samples were subsequently washed with the same buffer and post-fixed using 1% osmium tetroxide for an additional 2 hours. Dehydration was executed using ascending ethanol concentrations (10% to 100%), with each step maintained for 15 minutes, then immersed in absolute ethanol for 30 minutes. Resin infiltration was performed gradually with a mixture of epoxy resin and acetone before complete embedding in pure resin. Ultrathin sections were cut, mounted onto copper grids, and contrasted

with uranyl acetate followed by lead citrate staining. The prepared sections were visualized using a transmission electron microscope (JEOL-JEM 1010, 80 kV) available at the Regional Center for Mycology and Biotechnology (RCMB) [19].

Statistical analysis

All quantitative data were displayed as means accompanied by standard errors (SE). Statistical interpretation of the results was conducted using SPSS software, version 23. Differences between experimental groups were determined by applying one-way analysis of variance (ANOVA), followed by Tukey's post-hoc test for multiple comparisons. A significance threshold was set at $P < 0.05$ to determine statistical relevance [20].

Results and Discussion

Cytotoxicity

The cytotoxic effects of heliomycin and tamoxifen were evaluated through the MTT assay, which revealed different IC₅₀ values against MCF-7 cell lines, with varying toxicity observed. Both bleomycin and tamoxifen demonstrated notable toxicity toward the MCF-7 cells (**Figures 1a and 1b**). Interestingly, heliomycin exhibited greater toxicity compared to tamoxifen (**Figure 1c**). The IC₅₀ values for heliomycin and tamoxifen were found to be 18.87 $\mu\text{g/ml}$ and 29.6 $\mu\text{g/ml}$, respectively.

The MTT assay provided insight into the toxicity of the compounds, showing that cell viability significantly decreased, with a dose-dependent response observed. The untreated control cells maintained their typical morphology and behavior. The IC₅₀ values, indicating the concentrations required to reduce cell viability by 50%, revealed a marked difference in the lethal effects between heliomycin and tamoxifen on MCF-7 cells, even at the highest concentrations tested. After treatment, the cell shape altered to become thin and elongated. Compared to the untreated cells, which were more clustered, the tamoxifen-treated cells formed aggregates that were absent in the heliomycin-treated cells after exposure to their respective IC₅₀ concentrations. Several morphological abnormalities were observed, including cell rounding and areas where no cells were present (**Figure 1d**).

Cytopathology

Analysis using the H&E staining technique revealed notable changes, including a decrease in nuclear size, often associated with varying levels of chromatin condensation in the same culture. Apoptotic bodies displayed smaller cell sizes and the formation of blebs on the cell surface (**Figure 2**).

Immunocytochemistry

Immunocytochemistry results indicated significant differences in the intensity of color observed between treated and untreated cells due to the CK-19 immuno-antigen-antibody interaction. Both heliomycin- and tamoxifen-treated cells showed reduced CK-19 expression levels compared to the control (**Figure 3**).

Transmission electron microscopy

- In the control cells, the ultrastructural analysis revealed an abnormally large and irregular nucleus, with chromatin at the periphery and an expanded nucleolus (**Figure 3D a**).
- For heliomycin-treated cells, the ultrastructure showed signs of degeneration, including reduced nuclear size, with fragmented chromatin (**Figure 3D b**).
- In tamoxifen-treated cells, ultrastructural changes included cell degeneration, condensed nuclei, fragmented chromatin, and a noticeably enlarged and denser nucleolus (**Figure 3D c**).

Real-time PCR

Gene expression analysis of pro-apoptotic markers (TNF α , P53, and TLR4) and anti-apoptotic markers (HER-2 and ER α) in cells treated with heliomycin and tamoxifen revealed distinct expression patterns. HER-2 expression was found to be less elevated in tamoxifen-treated cells compared to heliomycin-treated cells and the control. P53 expression was significantly increased in heliomycin-treated cells, in contrast to tamoxifen-treated cells, when compared to the positive control. On the other hand, the expression of ER α , TNF α , and TLR4 was notably downregulated in heliomycin-treated cells compared to tamoxifen-treated cells and the positive control (**Figure 4**).

Flow cytometry and cell cycle analysis

Flow cytometry analysis indicated a marked increase in both early and late apoptotic cells in the tamoxifen and heliomycin treatment groups compared to the untreated cells. Specifically, tamoxifen-treated cells showed 5.66% early apoptosis and 11.16% late apoptosis, while heliomycin-treated cells had 3.22% and 14.46%, respectively. In contrast, the untreated cells showed only 0.27% early apoptosis and 0.15% late apoptosis. A slight increase in necrotic cells was also observed in both treated groups compared to the control MCF-7 cells (**Figure 5**).

Regarding the cell cycle, both treated groups displayed a significant increase in the Sub G1 phase, which corresponded with a notable decrease in the G0/G1 phase, compared to untreated cells. The S phase showed a minor decrease in both treated groups. Furthermore, the G2/M phase was significantly higher in the heliomycin-treated group compared to the tamoxifen-treated group when compared to the control. The untreated cells exhibited 1.78%, 52.06%, 39.88%, and 8.06% in the Sub G1, G0/G1, S, and G2/M phases, respectively. In contrast, heliomycin-treated cells showed 25.72%, 36.25%, 31.48%, and 38.27%, while tamoxifen-treated cells exhibited 23.14%, 38.45%, 36.99%, and 24.56% in the same phases (**Figures 5 and 6**).

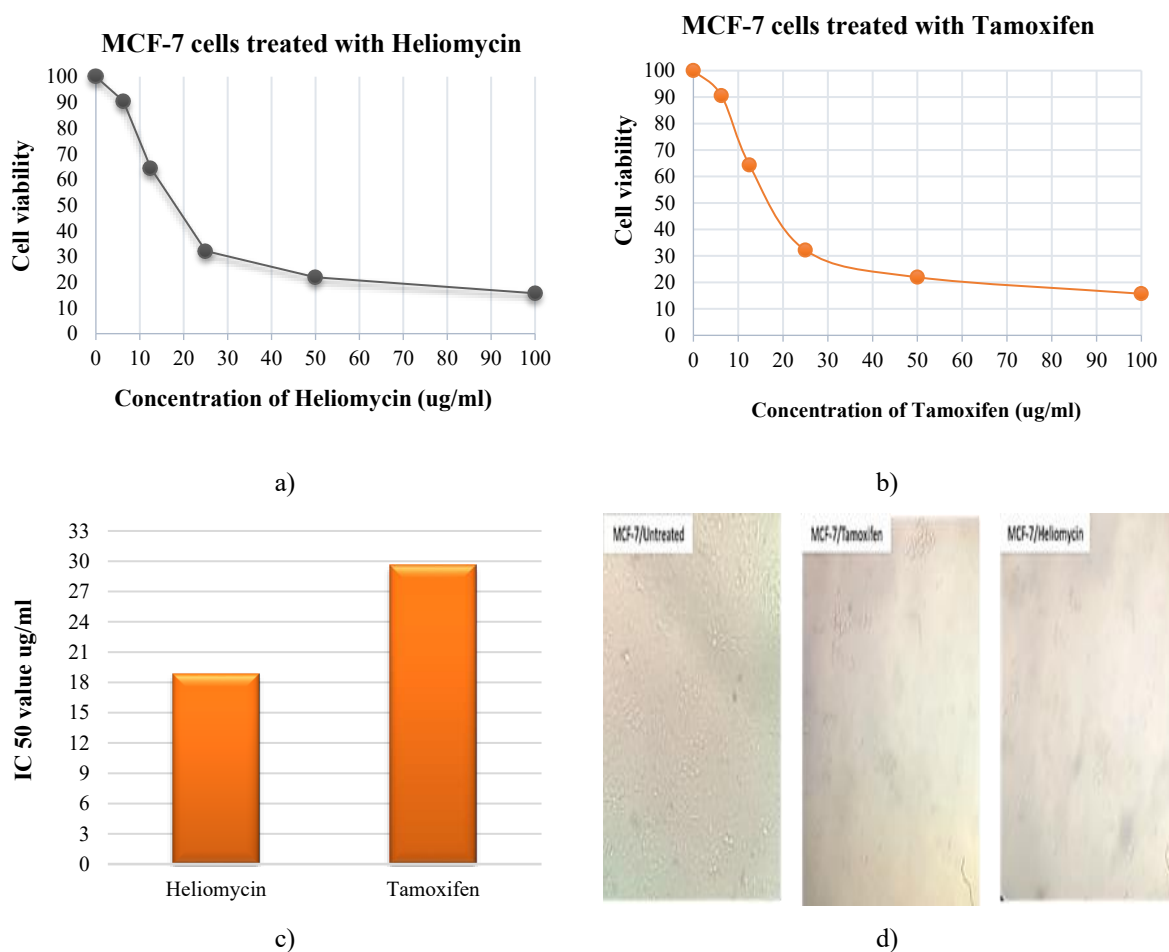
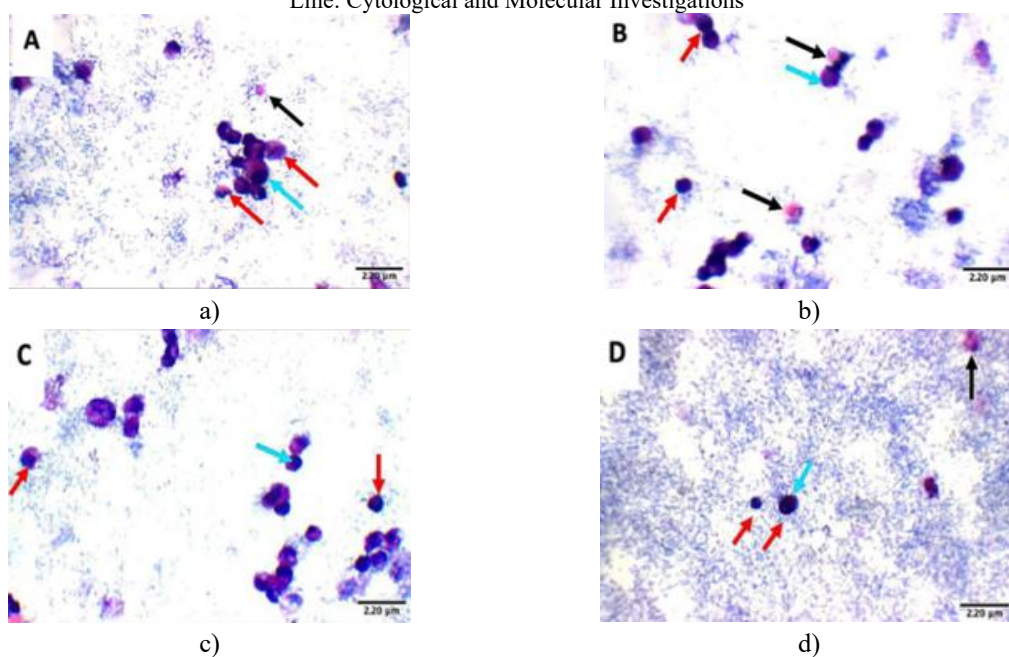
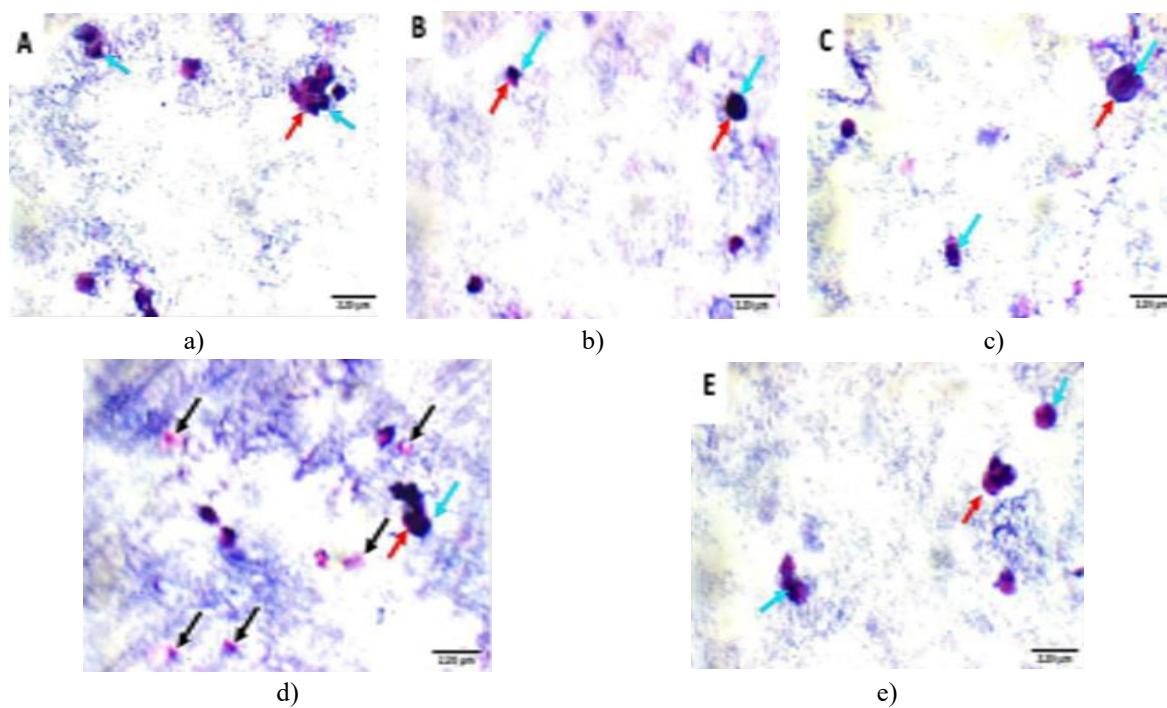


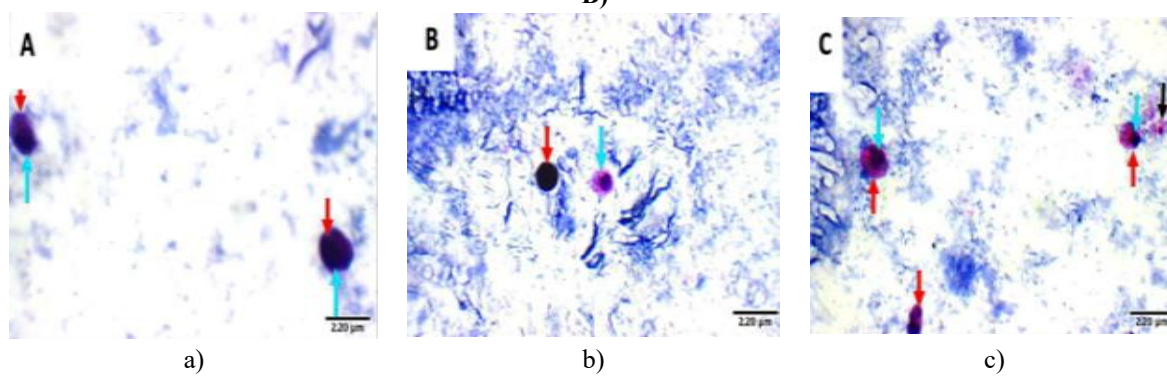
Figure 1. a) measurement of IC50 and the relationship between heliomycin concentrations and MCF-7 cell viability, b) measurement of IC50 and the relationship between tamoxifen concentrations and MCF-7 cell viability, c) evaluation of IC50 values for heliomycin and tamoxifen on MCF-7 cells using the MTT assay, and d) cytotoxic impact of heliomycin and tamoxifen on MCF-7 cells.



A)



B)



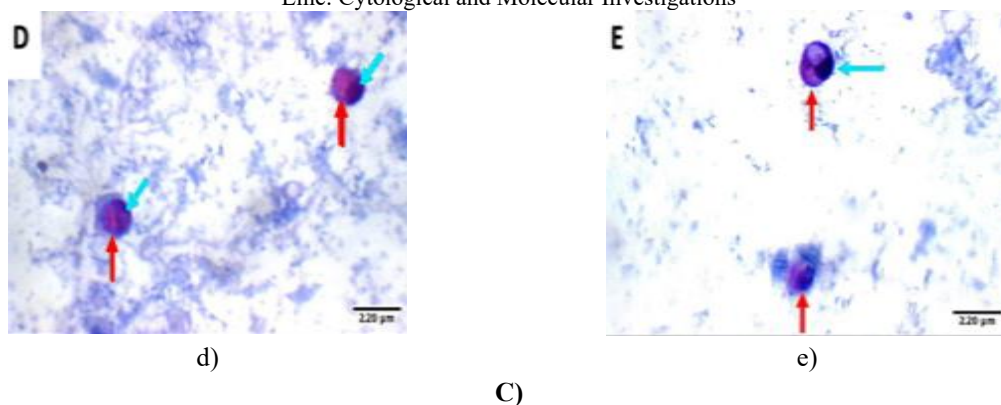
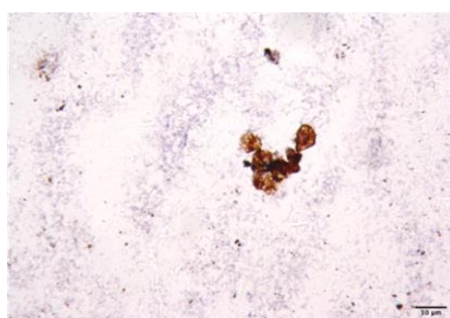
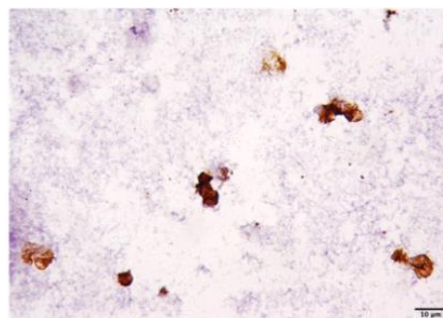


Figure 2. (A) Cytopathology of MCF-7 (positive control): (a) presence of clusters and isolated viable cells exhibiting marked pleomorphism (red arrow), with a higher nucleus-to-cytoplasm (N/C) ratio and hyperchromatic nuclei (blue arrow), along with one apoptotic cell per high-power field (HPF, black arrow), (b) another view with clusters and isolated viable cells showing marked pleomorphism (red arrow), hyperchromatic nuclei (blue arrow), and two apoptotic cells per HPF (black arrow), (c) additional view showing clusters and isolated viable pleomorphic cells (red arrow) with hyperchromatic nuclei (blue arrow), and (d) another angle showing isolated viable pleomorphic cells (red arrow) with hyperchromatic nuclei (blue arrow) and one apoptotic cell per HPF (black arrow) (H&E X400); (B) cytopathology of MCF-7 treated with tamoxifen: (a) clusters and isolated viable pleomorphic cells (red arrow) exhibiting an increased N/C ratio and hyperchromatic nuclei (blue arrow), (b) a different angle showing clusters and isolated viable cells with a high N/C ratio and hyperchromatic nuclei (blue arrow), (c) a further view showing isolated viable pleomorphic cells (red arrow) with elevated N/C ratio and hyperchromatic nuclei (blue arrow), (d) additional perspective displaying clusters and isolated viable cells (red arrow) with a high N/C ratio and hyperchromatic nuclei (blue arrow), and five apoptotic cells per HPF (black arrow), and (e) A final view showing isolated viable pleomorphic cells (red arrow) with a high N/C ratio and hyperchromatic nuclei (blue arrow), along with one apoptotic cell per HPF (black arrow) (H&E X400); (C) cytopathology of MCF-7 treated with heliomycin: (a) isolated viable pleomorphic cells (red arrow) showing a high N/C ratio and hyperchromatic nuclei (blue arrow), (b) another view displaying a viable cell with a high N/C ratio and hyperchromatic nuclei (red arrow), and another cell with hyperchromatic nuclei and eosinophilic cytoplasm (blue arrow), (c) additional view showing isolated viable pleomorphic cells (red arrow) with elevated N/C ratio and hyperchromatic nuclei (blue arrow), and one apoptotic cell per HPF (black arrow), (d) a further perspective showing isolated viable pleomorphic cells (red arrow) with an increased N/C ratio and hyperchromatic nuclei (blue arrow), and (e) another view displaying isolated viable pleomorphic cells (red arrow) with a high N/C ratio and hyperchromatic nuclei (blue arrow) (H&E X400).



a)



b)

A)

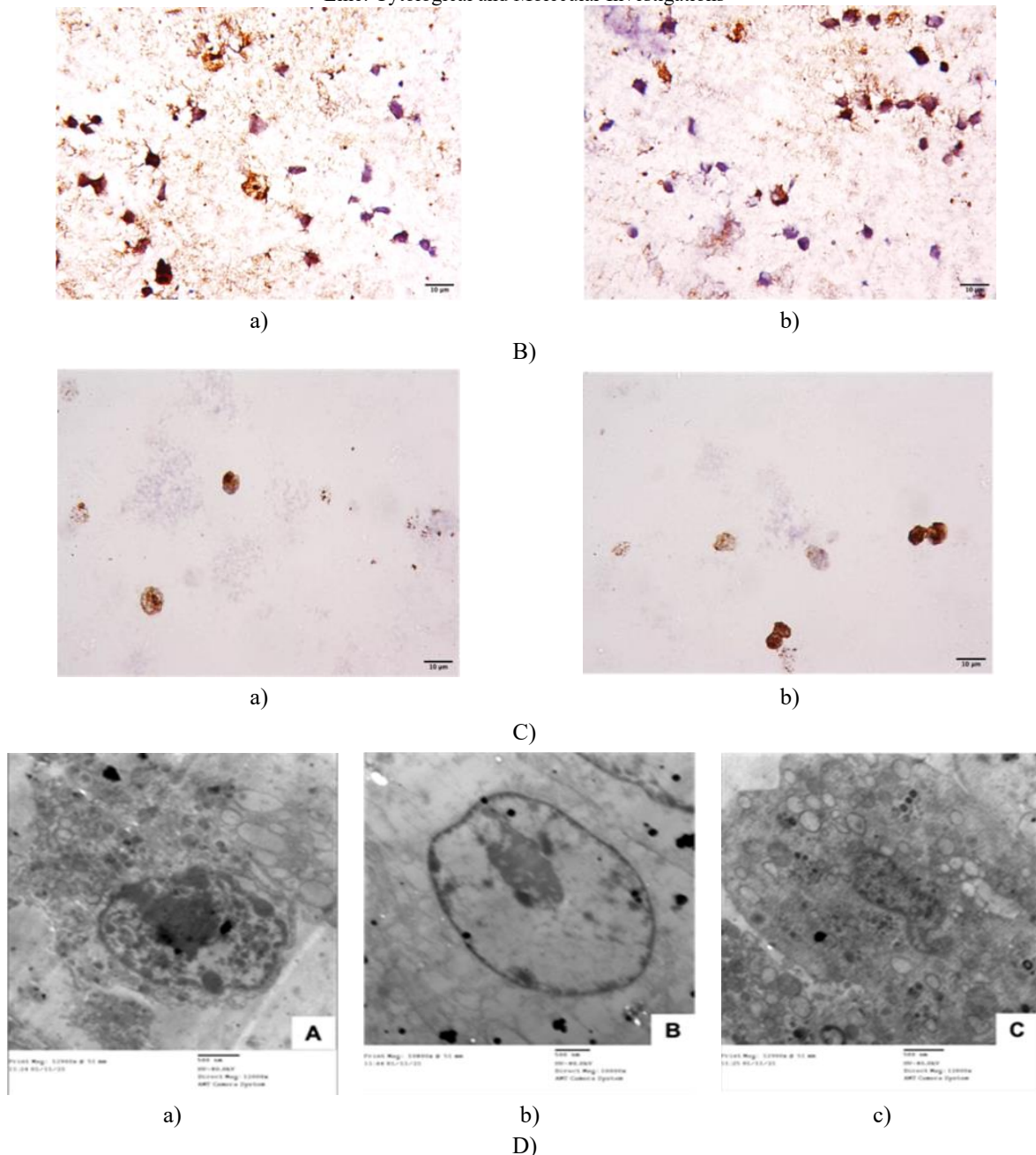


Figure 3. Immunocytochemistry and electron microscopy of MCF-7; (A) immunocytochemistry of MCF-7 adenocarcinoma cells: the MCF-7 cell clusters demonstrated intense staining for cyokeratin 19 (CK-19), (B) immunocytochemistry of tamoxifen-treated MCF-7 cells: tamoxifen-treated cells showed moderate expression of cyokeratin 19 (CK-19), (C) immunocytochemistry of heliomycin-treated MCF-7 cells: cells treated with heliomycin displayed low expression of cyokeratin 19 (CK-19); (D) transmission Electron Microscopy (TEM) of MCF-7: (a) control cells exhibited an enlarged and irregularly shaped nucleus, peripheral chromatin, and a significantly enlarged nucleolus, (b) tamoxifen-treated cells revealed degenerated morphology, with a shrunken nucleus, fragmented chromatin, and a densely enlarged nucleolus, and (c) heliomycin-treated cells demonstrated degeneration, with a shrunken nucleus and fragmented chromatin.

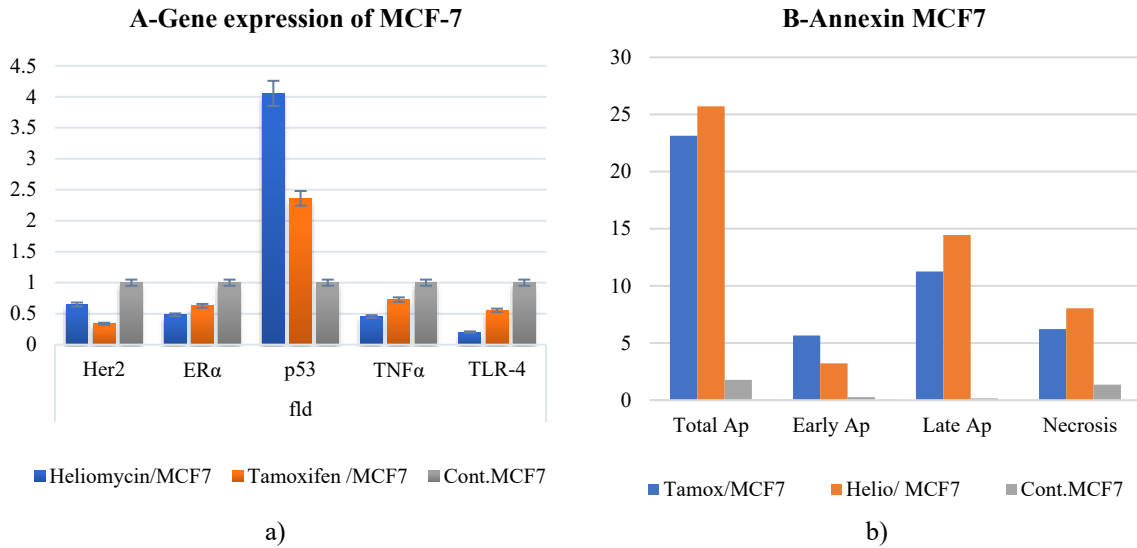


Figure 4. a) expression levels of HER-2, ER α , P53, TNF α , and TLR-4 in MCF-7 cells after treatment with heliomycin and tamoxifen, compared to the positive control, and b) evaluation of apoptosis and necrosis in MCF-7 cells using flow cytometry assay.

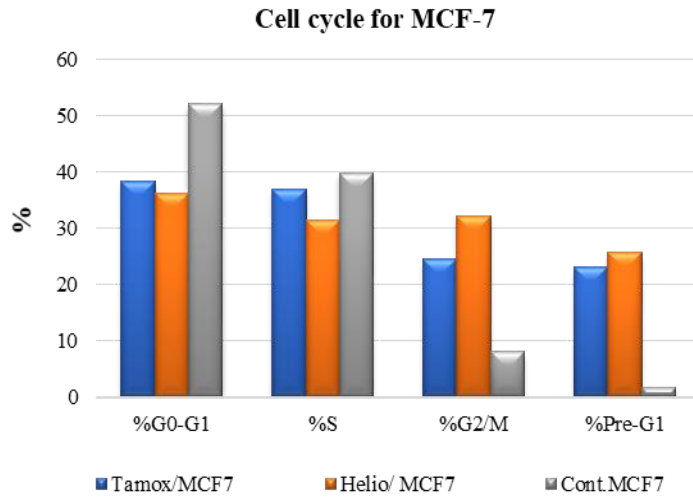
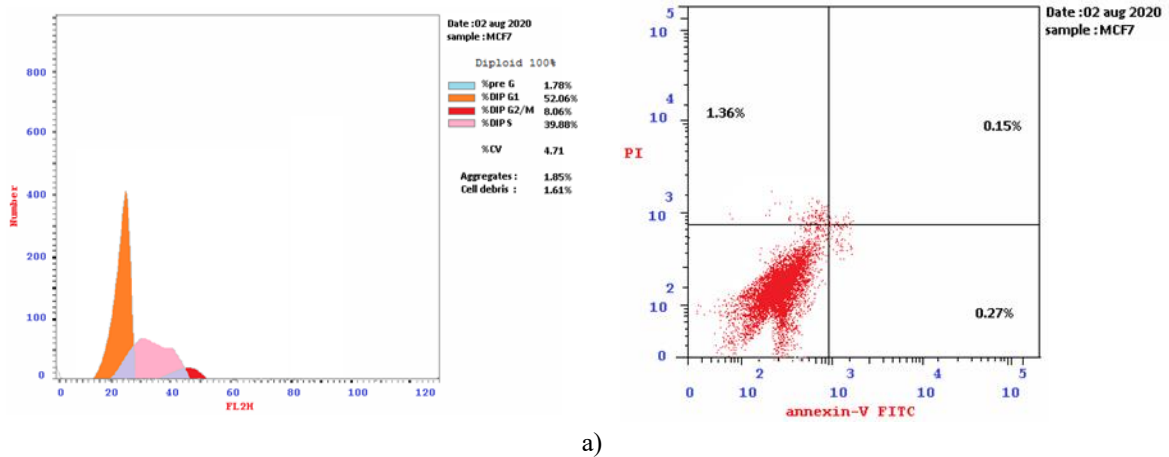


Figure 5. Analysis of the cell cycle distribution in MCF-7 cells using flow cytometry.



a)

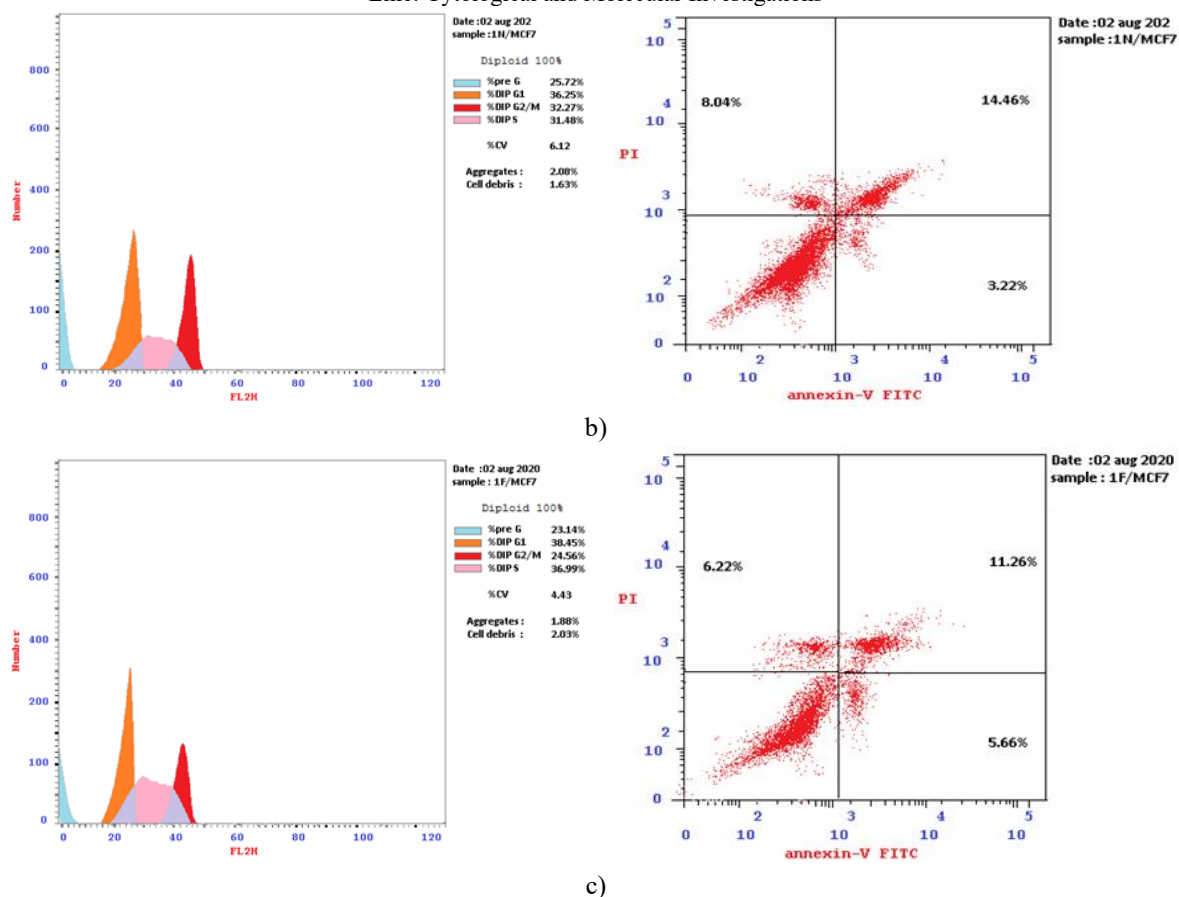


Figure 6. Flow cytometric analysis of the cell cycle distribution and apoptosis percentage in MCF-7 cells after treatment: (a) control group, (b) heliomycin-treated group, and (c) tamoxifen-treated group.

Breast cancer remains the leading cancer type among women worldwide and stands as the second most common cause of cancer mortality, just after lung cancer [21]. Natural product extracts are widely regarded as promising sources for new cancer treatment options.

In this study, we examined the effects of heliomycin and tamoxifen on MCF-7 breast cancer cells. The impact of these agents was analyzed through various methods including cell cycle analysis, apoptosis detection by flow cytometry, real-time RT-PCR for ER- α , HER-2, p53, TNF α , and TLR4 expressions, as well as cytopathological and immunocytochemical assessments.

Heliomycin, an aromatic polyketide compound, is recognized for its anticancer [22], antiviral, and antibacterial properties. Previous studies have demonstrated its ability to inhibit RNA polymerase [23], translation, and histone deacetylase [24]. The inhibition of histone deacetylase impairs DNA replication, halts the cell cycle, and stimulates apoptotic mechanisms.

Tamoxifen is a nonsteroidal drug with anti-estrogenic activity, often prescribed in the treatment of estrogen receptor-positive breast cancer [6]. It competes with estrogen for binding to its receptors, forming a complex that prevents DNA synthesis and disrupts estrogen-driven cell actions.

We initially determined the IC₅₀ values as a reference point for subsequent analyses. Our results indicated that heliomycin exhibited an IC₅₀ of 18.87 μ g/mL in MCF-7 cells, while tamoxifen showed a higher IC₅₀ of 29.6 μ g/mL. These values align with findings from Barba-Ostria *et al.* [25], who suggested that IC₅₀ values under 30 μ g/mL are crucial for identifying effective anticancer agents.

Extracts from actinomycetes, including cell-free extracts, are known to possess anticancer activity due to the presence of quinines and alkaloids in their metabolites [26]. These extracts have been shown to trigger apoptosis, disrupt fusion transcript degradation, encourage cellular differentiation, and reduce angiogenesis and proliferation [27].

CK19, a cytoskeletal protein expressed in epithelial cells, is also found in active tumor cells and metastatic breast cancer [28]. It is widely used as a marker for breast epithelial cell detection [29]. In our study, we observed varying degrees of CK-19 expression in MCF-7 cells: mild expression following heliomycin treatment, moderate

expression after tamoxifen treatment, and strong expression in the positive control group. Our findings are consistent with the work of Tanvetthayanont *et al.* [30], who reported that CK-19 expression increases in stages II and III of breast cancer, and Ghani *et al.* [31], who found CK-19 expression in MCF-7 and T47D cell lines, which are derived from luminal epithelial cells.

These findings suggest a direct relationship between CK-19 expression and the oncogenic activity of MCF-7 cells. Both heliomycin and tamoxifen showed significant anticancer effects, evidenced by their ability to reduce CK-19 expression compared to the positive control, where CK-19 expression remained high without any anticancer effects.

TNF- α is a pleiotropic cytokine that was originally identified for its role in inducing apoptosis in some cancer types but is also involved in promoting tumor growth. It can stimulate cellular transformation, proliferation, angiogenesis, invasion, and metastasis [32]. High levels of TNF- α are often found in various malignancies, especially in breast cancer, where it is associated with aggressive tumor behavior and a poor prognosis [33].

In our research, we observed a notable reduction in TNF- α levels in MCF-7 cells treated with heliomycin and tamoxifen when compared to untreated control cells. These findings are consistent with the work of Mocellin *et al.* [34], who reported that TNF- α levels are typically elevated in human epithelial cancers. In MCF-7 cells, TNF- α activates TNFR1, which then stimulates both JNK and PI3K/AKT pathways, leading to the activation of NF- κ B. This results in the upregulation of cyclin D1 and enhanced cell proliferation [34, 35]. Similar effects were observed when estradiol was applied [34]. Furthermore, TNF- α contributes to the growth of cancer cells by activating the p42/p44 MAPK pathway, which operates independently of NF- κ B and is regulated by TNFR1 and TNFR2, providing an additional mechanism for cancer progression [35]. While the JNK pathway makes MCF-7 cells more susceptible to apoptosis triggered by TNF- α , the p42/p44 MAPK remains minimally engaged [36].

Toll-like receptors (TLRs) are predominantly expressed in epithelial and immune cells and play a key role in triggering inflammatory responses by stimulating the production of cytokines [37, 38]. TLR4 expression in metastatic ductal carcinoma has been closely linked to clinical outcomes [39, 40]. In the current study, we found a reduction in TLR4 expression in MCF-7 cells treated with heliomycin and tamoxifen, in contrast to the untreated control cells. This aligns with the observations of Haricharan and Brown [41], who indicated that TLR4 modulates the balance between growth and apoptotic cytokines in TP53 mutant breast cancer cells, contributing to increased proliferation. Similarly, Yang *et al.* [42] found that TLR4 was expressed in MCF-7 and MDA-MB-231 cells.

The p53 protein, which regulates numerous cellular functions including the cell cycle, DNA repair, and immune response [42, 43], showed significant upregulation in MCF-7 cells treated with heliomycin and tamoxifen, compared to controls. This finding corroborates the study by Van Slooten *et al.* [44], who noted that increased mutations and reduced expression of p53 are often associated with higher proliferative potential in cancer cells.

HER2, a receptor in the epidermal growth factor receptor (EGFR) family, encodes a 185-kDa transmembrane protein found on chromosome 17 [44]. Our findings indicated a substantial decrease in HER2 expression in MCF-7 cells treated with heliomycin and tamoxifen, compared to controls. This is in line with Hudis [45], who reported that HER2 is overexpressed in 20-30% of breast cancer cases and is associated with poor prognosis, higher recurrence rates, and aggressive tumor behavior [46].

Estrogen, through its receptor (ER), plays a pivotal role in mammary gland development and has become a crucial target in treating luminal breast cancer [47]. In line with this, antiestrogen therapies such as tamoxifen and fulvestrant directly target ER signaling pathways [48]. The present research revealed a significant reduction in ER α expression in MCF-7 cells treated with heliomycin and tamoxifen, in agreement with [49], who found that elevated estrogen levels contribute to breast cancer progression.

Both tamoxifen and heliomycin were effective in inducing apoptosis and inhibiting the proliferation of MCF-7 cells. In tamoxifen-treated cells, we observed clusters of viable, highly pleomorphic cells with increased nuclear-to-cytoplasmic ratio (N/C ratio), hyperchromatic nuclei, and 1-6 apoptotic cells per high-power field (HPF). Helio-mycin-treated cells showed isolated viable cells with hyperchromatic nuclei and eosinophilic cytoplasm, as well as 1 apoptotic cell per HPF. The positive control cells exhibited clusters of viable cells with hyperchromatic nuclei, an elevated N/C ratio, and 1-2 apoptotic cells per HPF. These observations are consistent with those of Ahmad [21], who reported that heliomycin significantly inhibits the growth of various cancer cell lines, including HeLa, HepG2, and HMO2.

Molecular docking studies suggest that heliomycin may target HER2 tyrosine kinase, which is frequently overexpressed in cancer cells [49]. Additionally, heliomycin has been shown to modulate the balance between pro- and anti-apoptotic effects in cancer cells [46].

Apoptosis is characterized by distinct morphological changes, including cell shrinkage, fragmentation into apoptotic bodies, chromatin condensation, and DNA fragmentation [47, 48]. In our research, TEM analysis revealed that control MCF-7 cells exhibited enlarged and irregular nuclei, peripheral chromatin, and enlarged nucleoli. In contrast, heliomycin-treated cells showed degenerated morphology with shrunken nuclei and fragmented chromatin, while tamoxifen-treated cells displayed similar degenerative changes with dense nucleoli. These TEM findings support the conclusions drawn from cytopathological and flow cytometric analyses, indicating that both tamoxifen and heliomycin induce anticancer effects through the promotion of apoptosis [49].

Conclusion

Heliomycin, derived from actinomycetes bacteria, shows promising anticancer properties against MCF-7 breast cancer cells by promoting cell apoptosis and enhancing the expression of tumor-suppressing genes. This suggests its potential as an alternative or complementary therapeutic option alongside traditional chemotherapy treatments such as tamoxifen.

Acknowledgments: None

Conflict of Interest: None

Financial Support: None

Ethics Statement: None

References

1. Moslemi M, Moradi Y, Dehghanbanadaki H, Afkhami H, Khaledi M, Sedighimehr N, et al. The association between ATM variants and risk of breast cancer: a systematic review and meta-analysis. *BMC Cancer*. 2021;21(1):27.
2. Cao W, Chen HD, Yu YW, Li N, Chen WQ. Changing profiles of cancer burden worldwide and in China: a secondary analysis of the global cancer statistics 2020. *Chin Med J*. 2021;134(07):783-91.
3. Ikhuoria E, Bach C. Introduction to breast carcinogenesis – symptoms, risks factors, treatment, and management. *Eur J Eng Res Sci*. 2018;3(7):58.
4. Waks A, Winer E. Breast cancer treatment. *JAMA*. 2019;321(3):288.
5. Al-Zharani M, Nasr FA, Abutaha N, Alqahtani AS, Noman OM, Mubarak M, et al. Apoptotic induction and anti-migratory effects of *Rhazya stricta* fruit extracts on a human breast cancer cell line. *Molecules*. 2019;24(21):3968.
6. Shahbaz K. Tamoxifen: pharmacokinetics and pharmacodynamics. *Open Access J Pharm Res*. 2017;1(8).
7. Parthiban A, Sivasankar R, Sachithanandam V, Khan SA, Jayshree A, Murugan K, et al. An integrative review on bioactive compounds from Indian mangroves for future drug discovery. *S Afr J Bot*. 2022;149:899-915.
8. Budiyanoto F, Alhomaidi EA, Mohammed AE, Ghandourah MA, Alorfi HS, Bawakid NO, et al. Exploring the mangrove fruit: From the phytochemicals to functional food development and the current progress in the Middle East. *Mar Drugs*. 2022;20(5):303.
9. Bibi F, Azhar EI. Analysis of bacterial communities in sponges and coral inhabiting Red Sea, using barcoded 454 pyrosequencing. *Saudi J Biol Sci*. 2021;28(1):847-54.
10. Abdelfattah M, Elmallah M, Hawas U, Abou El-Kassem L, Eid M. Isolation and characterization of marine-derived actinomycetes with cytotoxic activity from the Red Sea coast. *Asian Pac J Trop Biomed*. 2016;6(8):651-7.
11. Chen J, Xu L, Zhou Y, Han B. Natural products from actinomycetes associated with marine organisms. *Mar Drugs*. 2021;19(11):629.
12. Elmallah M, Micheau O, Eid M, Hebishy A, Abdelfattah M. Marine actinomycete crude extracts with potent TRAIL-resistance overcoming activity against breast cancer cells. *Oncol Rep*. 2017;37(6):3635-42.

13. Ariabod V, Soholi M, Shekouhi R, Payan K. Assessment of breast cancer immunohistochemical properties with demographics and pathological features; a retrospective study. *Int J Cancer Manag.* 2021;14(11):e114577.
14. He S, Li Q, Huang Q, Cheng J. Targeting protein kinase C for cancer therapy. *Cancers.* 2022;14(5):1104.
15. Theodossiou T, Ali M, Grigalavicius M, Grallert B, Dillard P, Schink K, et al. Simultaneous defeat of MCF7 and MDA-MB-231 resistances by a hypericin PDT–tamoxifen hybrid therapy. *Npj Breast Cancer.* 2019;5(1):13.
16. Yumnam S, Hong G, Raha S, Saralamma V, Lee H, Lee W, et al. Mitochondrial dysfunction and Ca²⁺ overload contributes to hesperidin induced paraptosis in hepatoblastoma cells, HepG2. *J Cell Physiol.* 2016;231(6):1261-8.
17. Abdelfattah M, Ishikawa N, Karmakar U, Ishibashi M. Sulfotanone, a new alkyl sulfonic acid derivative from *Streptomyces* sp. IFM 11694 with TRAIL resistance-overcoming activity. *J Nat Med.* 2016;70(2):266-70.
18. Murad H, Hawat M, Ekhtiar A, AlJapawe A, Abbas A, Darwish H, et al. Induction of G1-phase cell cycle arrest and apoptosis pathway in MDA-MB-231 human breast cancer cells by sulfated polysaccharide extracted from *Laurencia papillosa*. *Cancer Cell Int.* 2016;16(1):1-1.
19. Amin BH, Abou-Dobara MI, Diab MA, Gomaa EA, El-Mogazy MA, El-Sonbati AZ, et al. Synthesis, characterization, and biological investigation of new mixed-ligand complexes. *Appl Organomet Chem.* 2020;34(8):e5689.
20. Nieminen P, Virtanen JI, Vähänikkilä H. An instrument to assess the statistical intensity of medical research papers. *PloS one.* 2017;12(10):e0186882.
21. Ahmad I. Recent developments in steroidal and nonsteroidal aromatase inhibitors for the chemoprevention of estrogen-dependent breast cancer. *Eur J Med Chem.* 2015;102:375-86.
22. Liu X, Arai MA, Ishibashi KT. Isolation of resistomycin from a terrestrial actinomycete with TRAIL resistance-overcoming activity. *Nat Prod Commun.* 2018;13(1):1934578X1801300119.
23. Martin II JK, Sheehan JP, Bratton BP, Moore GM, Mateus A, Li SH, et al. A dual-mechanism antibiotic kills gram-negative bacteria and avoids drug resistance. *Cell.* 2020;181(7):1518-32.
24. Abdelfattah MS, Elmallah MI, Faraag AH, Hebishy AM, Ali NH. Heliomycin and tetracinomycin D: anthraquinone derivatives with histone deacetylase inhibitory activity from marine sponge-associated *Streptomyces* sp. SP9. *3 Biotech.* 2018;8(6):1-9.
25. Barba-Ostria C, Carrera-Pacheco SE, Gonzalez-Pastor R, Heredia-Moya J, Mayorga-Ramos A, Rodríguez-Pólit C, et al. Evaluation of biological activity of natural compounds: current trends and methods. *Molecules.* 2022;27(14):4490.
26. Panggabean JA, Adiguna SB, Murniasih T, Rahmawati SI, Bayu A, Putra MY. Structure–activity relationship of cytotoxic natural products from Indonesian marine sponges. *Rev Bras Farmacogn.* 2022;32(1):12-38.
27. Davies-Bolorunduro OF, Adeleye IA, Akinleye MO, Wang PG. Anticancer potential of metabolic compounds from marine actinomycetes isolated from Lagos lagoon sediment. *J Pharm Anal.* 2019;9(3):201-8.
28. Saha SK, Kim K, Yang GM, Choi HY, Cho SG. Cytokeratin 19 (KRT19) has a role in the reprogramming of cancer stem cell-like cells to less aggressive and more drug-sensitive cells. *Int J Mol Sci.* 2018;19(5):1423.
29. Zhang S, Jiang H, Gao B, Yang W, Wang G. Identification of diagnostic markers for breast cancer based on differential gene expression and pathway network. *Front Cell Dev Biol.* 2022;9:3760.
30. Tanvetthayanont P, Yata T, Boonnil J, Temisak S, Ponglowhapan S. Validation of droplet digital PCR for cytokeratin 19 mRNA detection in canine peripheral blood and mammary gland. *Sci Rep.* 2022;12(1):13623.
31. Ghani FI, Dendo K, Watanabe R, Yamada K, Yoshimatsu Y, Yugawa T, et al. An ex-vivo culture system of ovarian cancer faithfully recapitulating the pathological features of primary tumors. *Cells.* 2019;8(7):644.
32. Mercogliano MF, Bruni S, Elizalde PV, Schillaci R. Tumor necrosis factor α blockade: an opportunity to tackle breast cancer. *Front Oncol.* 2020;10:584.
33. Haid PP, Terkawal SU, Zakaria Z, AB Hamid WZ, Mohamed M. Tualang honey supplementation improves inflammatory and bone markers among postmenopausal breast cancer patients: a randomised controlled trial. *Sains Malays.* 2021;50(7):1971-85.
34. Mocellin D, Bratti LD, Silva AH, Assunção LS, Kretzer IF, Filippin-Monteiro FB. Serum from morbidly obese patients affects melanoma cell behavior in vitro. *Braz J Pharm Sci.* 2022;58(8):e19375.

35. Starek-Świechowicz B, Budziszewska B, Starek A. Endogenous estrogens—breast cancer and chemoprevention. *Pharmacol Rep.* 2021;73(6):1497-512.
36. Rivas MA, Carnevale RP, Proietti CJ, Rosembli C, Beguelin W, Salatino M, et al. TNF α acting on TNFR1 promotes breast cancer growth via p42/P44 MAPK, JNK, Akt and NF- κ B-dependent pathways. *Exp Cell Res.* 2008;314(3):509-29.
37. Jupp OJ, McFarlane SM, Anderson HM, Littlejohn AF, Mohamed AA, MacKay RH, et al. Type II tumour necrosis factor- α receptor (TNFR2) activates c-Jun N-terminal kinase (JNK) but not mitogen-activated protein kinase (MAPK) or p38 MAPK pathways. *Biochem J.* 2001;359(3):525-35.
38. Brubaker SW, Bonham KS, Zanoni I, Kagan JC. Innate immune pattern recognition: a cell biological perspective. *Ann Rev Immunol.* 2015;33(1):257-90.
39. Johnston DG, Corr SC. Toll-like receptor signalling and the control of intestinal barrier function. *Toll-Like Receptors: Practice and Methods.* 2016:287-300.
40. Ehsan N, Murad S, Ashiq T, Mansoor MU, Gul S, Khalid S, et al. Significant correlation of TLR4 expression with the clinicopathological features of invasive ductal carcinoma of the breast. *Tumor Biol.* 2013;34:1053-9.
41. Haricharan S, Brown P. TLR4 has a TP53-dependent dual role in regulating breast cancer cell growth. *Proc Natl Acad Sci.* 2015;112(25):E3216-25.
42. Yang H, Wang B, Wang T, Xu L, He C, Wen H, et al. Toll-like receptor 4 prompts human breast cancer cells invasiveness via lipopolysaccharide stimulation and is overexpressed in patients with lymph node metastasis. *PLoS one.* 2014;9(10):e109980.
43. Denisenko TV, Pivnyuk AD, Zhivotovsky B. p53-autophagy-metastasis link. *Cancers.* 2018;10(5):148.
44. Van Slooten HJ, Van De Vijver MJ, Børresen AL, Eyfjörd JE, Valgardsdóttir R, Scherneck S, et al. Mutations in exons 5–8 of the p53 gene, independent of their type and location, are associated with increased apoptosis and mitosis in invasive breast carcinoma. *J Pathol.* 1999;189(4):504-13.
45. Hudis CA. Trastuzumab—mechanism of action and use in clinical practice. *N Engl J Med.* 2007;357(1):39-51.
46. Meric-Bernstam F, Hung MC. Advances in targeting human epidermal growth factor receptor-2 signaling for cancer therapy. *Clin Cancer Res.* 2006;12(21):6326-30.
47. Alhuzaim W, Alosaimi M, Almesfer AM, Al Shahrani NM, Alali AH, Alibrahim KI, et al. Saudi patients' knowledge, behavior, beliefs, self-efficacy and barriers regarding colorectal cancer screening. *Int J Pharm Res Allied Sci.* 2020;9(1):14-20.
48. Babaei H, Sepahy AA, Amini K, Saadatmand S. The effect of titanium dioxide nanoparticles synthesized by bacillus tequilensis on clb gene expression of colorectal cancer-causing Escherichia coli. *Arch Pharm Pract.* 2020;11(1):22-31.
49. Algarni SB, Alsugair MM, Alkhars MK, Addas MJ, Hakeem MA, AlSalman AA, et al. Evaluation role of imaging studies in the staging of breast cancer. *Arch Pharm Pract.* 2020;11(4):70-5.